



HAL
open science

Antibody-coated microbiota in nasopharynx of healthy individuals and hypogammaglobulinemia patients.

Pedro Goncalves, Bruno Charbit, Christelle Lenoir, Darragh Duffy, Alain Fischer, James Di Santo

► To cite this version:

Pedro Goncalves, Bruno Charbit, Christelle Lenoir, Darragh Duffy, Alain Fischer, et al.. Antibody-coated microbiota in nasopharynx of healthy individuals and hypogammaglobulinemia patients.. 2020. pasteur-02456258

HAL Id: pasteur-02456258

<https://pasteur.hal.science/pasteur-02456258>

Preprint submitted on 27 Jan 2020

HAL is a multi-disciplinary open access archive for the deposit and dissemination of scientific research documents, whether they are published or not. The documents may come from teaching and research institutions in France or abroad, or from public or private research centers.

L'archive ouverte pluridisciplinaire **HAL**, est destinée au dépôt et à la diffusion de documents scientifiques de niveau recherche, publiés ou non, émanant des établissements d'enseignement et de recherche français ou étrangers, des laboratoires publics ou privés.

Journal Pre-proof

Antibody-coated microbiota in nasopharynx of healthy individuals and hypogammaglobulinemia patients.

Pedro Goncalves, PhD, Bruno Charbit, MSc, Christelle Lenoir, MSc, the Milieu Interieur Consortium, Darragh Duffy, PhD, Alain Fischer, MD, PhD, James P. Di Santo, MD, PhD

PII: S0091-6749(20)30036-1

DOI: <https://doi.org/10.1016/j.jaci.2020.01.002>

Reference: YMAI 14366

To appear in: *Journal of Allergy and Clinical Immunology*

Received Date: 24 October 2019

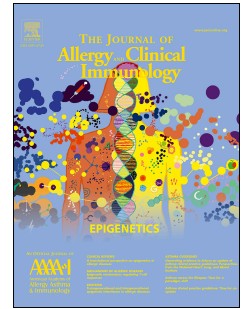
Revised Date: 2 January 2020

Accepted Date: 7 January 2020

Please cite this article as: Goncalves P, Charbit B, Lenoir C, the Milieu Interieur Consortium, Duffy D, Fischer A, Di Santo JP, Antibody-coated microbiota in nasopharynx of healthy individuals and hypogammaglobulinemia patients., *Journal of Allergy and Clinical Immunology* (2020), doi: <https://doi.org/10.1016/j.jaci.2020.01.002>.

This is a PDF file of an article that has undergone enhancements after acceptance, such as the addition of a cover page and metadata, and formatting for readability, but it is not yet the definitive version of record. This version will undergo additional copyediting, typesetting and review before it is published in its final form, but we are providing this version to give early visibility of the article. Please note that, during the production process, errors may be discovered which could affect the content, and all legal disclaimers that apply to the journal pertain.

© 2020 Published by Elsevier Inc. on behalf of the American Academy of Allergy, Asthma & Immunology.



*Antibody-coated microbiota in nasopharynx of healthy individuals
and hypogammaglobulinemia patients.*

1 **Short title:** Ig coated bacteria in the human nasopharynx

2 Pedro Goncalves, PhD^{1,2}, Bruno Charbit, MSc³, Christelle Lenoir MSc⁴, the Milieu Interieur
3 Consortium, Darragh Duffy, PhD^{2,3,5}, Alain Fischer MD, PhD^{4,6,7,8} and James P Di Santo,
4 MD, PhD^{1,2}.

5

6

7 ¹Innate Immunity Unit, Institut Pasteur, Paris, France

8 ²Institut National de la Santé et de la Recherche Médicale (INSERM) U1223, Paris, France

9 ³Center for Translational Research, Institut Pasteur, Paris 75015, France

10 ⁴Institut National de la Santé et de la Recherche Médicale (INSERM) UMR 1163, Paris,
11 France.

12 ⁵Laboratory of Dendritic Cell Immunobiology, Department of Immunology, Institut Pasteur,
13 Paris 75015, France

14 ⁶University Paris Descartes Sorbonne Paris Cité, Imagine Institut, Paris, France.

15 ⁷Department of Pediatric Immunology, Hematology and Rheumatology, Necker-Enfants
16 Malades Hospital, Assistance Publique-Hôpitaux de Paris (APHP), Paris, France.

17 ⁸Collège de France, Paris, France.

18

19

20 ***Corresponding author:** Prof. James P Di Santo, MD, PhD, Innate Immunity Unit, Institut
21 Pasteur, 25 rue du Docteur Roux, 75724 Paris, France.; phone: +33-0145688209; e-mail:
22 james.di-santo@pasteur.fr

23 **Capsule summary:** We show that nasopharyngeal microbiota are coated by different
24 immunoglobulin isotypes in healthy individuals and with IgG in X-linked
25 agammaglobulinemia (XLA) patients treated with immunoglobulin replacement therapy.

26

27 **Key Words:** human nasopharynx microbiota; antibody-coated microbiota; sIgA; sIgM; IgD;
28 IgG; healthy; X-linked (Bruton's) agammaglobulinemia patients; Immunoglobulin (IgG)
29 replacement therapy; microbiota dysbiosis.

30

31 Disclosure of potential conflict of interest:

32 The authors declare that they have no relevant conflicts of interest.

33

34

35 To the Editor:

36 Respiratory diseases are important causes of death, which collectively account for
37 more than 1 in 10 of all deaths worldwide (WHO). Pathobionts, potential pathogenic bacteria
38 which under normal circumstances are present as harmless microorganisms, can be found
39 embedded in the nasopharyngeal commensal microbiota. Interestingly, the upper airway
40 microbiome composition seems very similar to that of the lung, and pathobionts present in the
41 nasopharynx can be a primary source of lower respiratory tract infections¹. Several elements
42 participate in respiratory mucosal barrier against invasive pathobionts including the
43 commensal microbiota and glands that secrete and create an antimicrobial mucus barrier
44 containing antimicrobial peptides, immunoglobulins and other soluble factors. Secretory
45 immunoglobulin A (sIgA) and sIgM are transported through nasopharynx epithelial cells by
46 polymeric Ig receptor (pIgR), and IgG by neonatal FcR (FcRn). Transepithelial transport of
47 IgD has not been documented, but IgD is found in nasopharynx secretions² perhaps deriving
48 from paracellular diffusion through cell junctions.

49 sIgA is the predominant antibody isotype in human nasopharyngeal secretions and it is
50 assumed that the majority of sIgA targets the resident commensal microbiota, inhibiting their
51 penetration via agglutination within the mucus layer, thereby reinforcing commensalism and
52 increasing microbiota diversity³. High-affinity sIgA appears to neutralize microbial toxins and
53 invasive pathogens in the absence of complement fixation³. Interestingly, Fadallah *et al*⁴
54 reported recently that Selective IgA Deficiency (SIgADef) patients display mild dysbiosis
55 with expansion of some pathobiont species in their feces as compared to healthy controls,
56 although these patients are not abnormally susceptible to intestinal infections⁴. On the other

57 hand, recurrent pulmonary infections constitute the most prevalent comorbidity in SIgADef
58 patients⁴, suggesting that sIgA may have tissue-specific roles in immune defense, especially
59 in the respiratory tract. A better understanding of immunoglobulins coating nasopharynx
60 microbiota in healthy individuals could provide an important basis for the prevention of
61 respiratory illnesses in some cases of humoral immunodeficiency.

62 To better understand the role for IgA (and other Ig isotypes) in regulating
63 nasopharyngeal microbial communities, we analyze nasopharyngeal samples to detect Ig-
64 bound microbes followed by 16S ribosomal RNA (rRNA) sequencing (Ig-seq) to determine
65 the type of bacteria targeted by each Ig isotype. We stained nasopharyngeal samples with
66 anti-human IgA, IgM, IgD and IgG antibodies and measured the immunoglobulin-bound
67 populations using a flow cytometer-based assay⁵. The gating strategy for immunoglobulin
68 staining of human nasopharynx microbiota is shown in Fig E1 (all methods are described in
69 the Methods section in this article's Online Repository at www.jacionline.org). On average, a
70 majority of the nasopharynx microbiota appears targeted by sIgA in healthy subjects (Fig
71 E1A), although the frequency of sIgA⁺ microbes is highly variable between individuals (Fig
72 E1B). Next we performed flow sorting of IgA-bound nasopharyngeal microbiota followed by
73 16S rRNA sequencing (IgA-seq) on a fraction of samples (n=4) (Fig E2A). Beta diversity
74 shows the extent of difference in microbiota community composition from different
75 environments or conditions. The beta diversity, based on Bray-Curtis distance matrix and
76 subjected to Principle Coordinate Analysis, suggest that bacteria derived from IgA⁺ and IgA⁻
77 fractions cluster distinctly, however, permutational multivariate analysis of variance
78 (PERMANOVA) of the two fractions was not significantly different (Fig E2A, B). The alpha
79 diversity and the Shannon Diversity Index (a combined measure of evenness and number of
80 bacteria) was lightly decreased in 16S rRNA sequences derived from IgA⁻ fraction (Fig E2C).
81 However, both IgA⁺ and IgA⁻ fractions exhibited equal distributions of rare and abundant
82 genera and thus IgA appears to target nasopharyngeal commensals irrespective of their
83 frequency (Fig E2D). These results suggest that under homeostatic conditions, sIgA bind to a
84 broad repertoire of bacteria present in nasopharyngeal microbiota including both commensals
85 and pathobionts³.

86 Most SIgADef patients have a mild clinical phenotype⁴, which may result from the
87 ability of other Ig isotypes to functionally replace IgA. Increased IgD⁺IgM⁻ B cell populations
88 and increased soluble IgD levels have been described in healthy human upper respiratory
89 mucosa². Therefore, even if IgM and IgD have the same V region and the same antigen
90 specificity, nasopharynx/respiratory B cells apparently switch from IgM to secrete IgD,

91 suggesting some functional advantage of the latter. The IgD hinge region linking is longer and
92 more flexible than that of IgM thereby facilitating IgD binding to antigens at lower
93 concentrations and in immune complexes². Still, sIgM binds some residual bacteria in the
94 nasopharynx (Fig E1), suggesting that IgM may participate in microbiota agglutination in the
95 steady-state. On the other hand, we found that a vast majority (86%) of the nasopharynx
96 microbiota is targeted by secreted IgD in healthy individuals (Fig E1). We observed that up to
97 60% of nasopharynx microbiota are double SIgA⁺IgD⁺ coated (Fig 1A, B). We performed
98 flow sorting to isolate IgD-bound microbiota and 16S rRNA sequencing to identify the
99 microbes specifically targeted by IgD (Fig 1C). The IgD⁺ SIgA⁻ fraction showed a higher
100 microbial diversity as compared to SIgA⁺IgD⁻ (Fig 1D). The beta diversity based on Bray-
101 Curtis distances was also different (Fig 1E), suggesting that IgD bind specifically to bacteria
102 not targeted by SIgA. IgD⁺SIgA⁻ fraction exhibited an enrichment in *Proteobacteria* phyla
103 (including *Haemophilus* and *Moraxella* genus) and the pathobionts *Pseudomonas* and
104 *Escherichia-Shigella* (Fig 1F). Previous studies showed that IgD somatic hypermutation
105 (SHM) frequencies are correlated with higher rates of upper respiratory infection⁶, suggesting
106 that pathobiont exposures drive SHM of antigen experienced IgD⁺ B cells. Our results suggest
107 that IgD can recognize a diverse array of both commensal and pathobiont bacteria inhabiting
108 the human upper respiratory mucosa in a manner similar to sIgA. SIgA^{Def} patients have
109 increase in IgD-producing B cells in the upper respiratory mucosa and increased IgD
110 secretion², our results are consistent with the notion that IgD may provide a layer of mucosal
111 protection during IgA deficiency.

112 Several studies demonstrated that mice and human IgG can react to conserved
113 commensal antigens and coat both commensal and pathogenic bacteria⁷. However, Fadallah *et*
114 *al.*,⁵ recently showed that almost no bacteria in healthy human feces were coated with IgG.
115 Despite the “absence” of IgG coated bacteria in feces, IgG present in serum of these
116 individuals recognizes a wide range of commensals under homeostatic conditions⁵. In
117 addition, SIgA^{Def} patients have a increased anti-commensal IgG response⁵. The reduction in
118 IgG coated bacteria in feces does not exclude the possibility that IgG coated bacteria can be
119 present within gut mucus, because IgG have the ability to attach to mucus proteins (e.g.
120 mucin-bound IgG Fc binding protein)⁸. Significant quantities of IgG are secreted and detected
121 within the mucus layer of human respiratory tract and we found that approximately 70% of
122 the microbiota present in nasopharynx secretions are targeted by IgG in healthy individuals
123 (Fig E1). These results demonstrate that human IgG may opsonize a wide range of
124 nasopharynx microbiota under homeostatic conditions. 16S rRNA sequencing of IgG-bound

125 bacteria allowed identification of their taxonomy (Fig E3A). We observed that the IgG⁺
126 fraction have reduced alpha diversity (Shannon index) comparatively to the IgG⁻ fraction (Fig
127 E3B), suggesting that IgG bind selectively to their target and are less polyreactive than IgA.
128 The beta diversity based on Bray-Curtis distance was also significantly different in terms of
129 both abundance and presence/absence of different OTUs (Fig E3C). IgG⁺ fraction exhibited a
130 significant decrease in binding in different genera, especially from *Proteobacteria* phylum
131 (*Betaproteobacteria*, *Campylobacteriales*, *Enterobacteriales*, *Pseudomonadales*) (Fig E3D).
132 Members of *Proteobacteria* phylum are reported to be weak inducers of systemic IgG
133 responses⁵ and we found that IgG bind weakly to genera from *Proteobacteria* in nasopharynx
134 of healthy individuals. Using the double binding with IgA and IgG antibodies we observed
135 that about 54% of nasopharynx bacteria are double SIgA⁺IgG⁺ coated, and the level of IgG-
136 only coated is low (16%) (Fig E3E, F). This data suggest that 77% of microbiota normally
137 coated by SIgA are also coated with IgG, demonstrating a convergence of IgA and IgG
138 responses toward the same microbial targets under homeostatic conditions. Sequencing of
139 flow sorted IgG⁺SIgA⁻ and SIgA⁺IgG⁻ bacteria (Fig E3G) showed that alpha diversity
140 (Shannon index) (Fig E3H) and beta diversity (based on Bray-Curtis distance) (not showed)
141 were not significantly different between IgG⁺SIgA⁻ and SIgA⁺IgG⁻ fractions. We observed
142 only a small enrichment on *Bacteroidetes* on IgG-only coated fraction (Fig E3I). Previous
143 studies showed that human and mice IgG recognized *Bacteroides* that belongs to this
144 phylum⁷. However, we conclude that IgG recognizes a diverse array of both nasopharynx
145 pathobionts and commensal bacteria⁷. SIgADef patients have an increased anti-commensal
146 IgG response associated with reduced systemic inflammation⁵, our results are consistent with
147 the notion that IgG may provide a layer of mucosal protection during IgA deficiency.

148 Immunoglobulin (IgG) replacement therapy (IVIg) has been used extensively in the
149 treatment of primary and secondary immunodeficiency diseases. With IVIg therapy, X-linked
150 agammaglobulinaemia (XLA-BTK) patients (characterized by a near-complete lack of Igs)
151 have a significant reduction in the occurrence of respiratory tract infections and these patients
152 may live a relatively healthy life⁹. We next studied the immunoglobulins coating of
153 nasopharynx microbiota in IVIg treated XLA-BTK patients. XLA-BTK patients lack IgA,
154 IgM and IgD nasopharynx microbiota binding (Fig 2A). On the other hand, IVIg therapy
155 restore the secretion of nasopharynx IgG (not shown) and enhances IgG nasopharynx
156 microbiota binding (Fig 2A). However, despite this increase in IgG coating, XLA-BTK
157 patients exhibit nasopharyngeal microbiota dysbiosis. The beta diversity based on Bray-Curtis
158 distance was significantly different in terms of both abundance and presence/absence of

159 different OTUs (Fig 2B) and have also a low alpha microbial diversity (Shannon index)
160 comparatively to healthy individuals (Fig 2C). XLA-BTK patients exhibited a significant
161 enrichment in *Proteobacteria* phyla (Fig 2D) and different pathobiont genera, especially
162 *Streptococcus* (and *Streptococcus pneumoniae* specie, not shown), *Moraxella*, *Alloiococcus*,
163 *Bacteroides*, mucus-degrading *Mucispirillum* among others commensals (Fig 2F). For
164 example, IgG bind weakly to genera from *Proteobacteria* phylum in healthy (Fig E3D),
165 suggesting that the lack of IgA/IgD binding (Fig 1F)⁴ contributes to the *Proteobacteria* phyla
166 expansion in XLA BTK patients. These results suggest that IVIg (IgG) therapy can not fully
167 control pathobiont (e.g. *S. pneumoniae*) carriage load in nasopharyngeal cavity of XLA-BTK
168 patients. Our results suggest an incomplete efficacy of IVIg (IgG) therapy in these patients
169 (that may be related to the absence of IgA and IgM/IgD in these preparations) which raises
170 the subsequent risk of recurrent sinus and respiratory tract infections⁹. However, the present
171 study is consistent with a protective role of IgG antibodies in the nasopharyngeal mucosa in
172 the context of IgA, IgM and IgA deficiency. IVIg therapy can help in control respiratory
173 infections in primary immunodeficiency diseases patients by promoting pathogens
174 opsonization, inducing complement activation and activation of Fc receptors for IgG if the
175 opsonized bacteria reach the epithelium or the circulation to disseminate to systemic organs.
176 However, these patients might also benefit from prophylactic IgA administration.

177 *Pedro Goncalves, PhD^{a,b},*
178 *Bruno Charbit, MSc^c*
179 *Christelle Lenoir MSc^d,*
180 *the Milieu Interieur Consortium*
181 *Darragh Duffy, PhD^{b,c,e}*
182 *Alain Fischer MD, PhD^{d,f,g,h}*
183 *James P Di Santo, MD, PhD^{a,b}*

184 From ^aInnate Immunity Unit, Institut Pasteur, Paris, France; ^bInstitut National de la Santé et
185 de la Recherche Médicale (INSERM) U1223, Paris, France; ^cCenter for Translational
186 Research, Institut Pasteur, Paris 75015, France; ^dInstitut National de la Santé et de la
187 Recherche Médicale (INSERM) UMR 1163, Paris, France; ^eLaboratory of Dendritic Cell
188 Immunobiology, Department of Immunology, Institut Pasteur, Paris 75015, France;
189 ^fUniversity Paris Descartes Sorbonne Paris Cité, Imagine Institut, Paris, France; ^gDepartment
190 of Pediatric Immunology, Hematology and Rheumatology, Necker-Enfants Malades Hospital,

191 Assistance Publique-Hôpitaux de Paris (APHP), Paris, France; ^hCollège de France, Paris,
192 France.E-mail: james.di-santo@pasteur.fr

193

194 We thank the X-linked agammaglobulinaemia (XLA-BTK) patients and healthy donors that
195 provided samples used in this study. We thank the members of Biomics NGS platform of the
196 Institut Pasteur, Sean Kennedy and Laurence Motreff for microbial sequencing, and Amine
197 Ghazlane and for the assistance with the data analysis. We thank members of the Di Santo
198 laboratory for discussions. Labex Milieu Intérieur ANR 10-LBX-69-01 MI
199 (<http://www.milieuinterieur.fr/en>) funded this study and the researcher P. Gonçalves. This
200 study was also partially supported by grants from the Institut Pasteur, INSERM, and the
201 European Research Council (ERC) under the European Union's Horizon 2020 research and
202 innovation program (695467 - ILC_REACTIVITY).

203

204

205 REFERENCES

- 206 1. Bassis CM, Erb-Downward JR, Dickson RP, Freeman CM, Schmidt TM, Young VB, et al.
207 Analysis of the Upper Respiratory Tract Microbiotas as the Source of the Lung and Gastric
208 Microbiotas in Healthy Individuals. *MBio*. 2015; 6:e00037.
- 209 2. Chen K, Cerutti A. New insights into the enigma of immunoglobulin D. *Immunological*
210 *Reviews* 2010; 237:160-79.
- 211 3. Jorgensen SF, Holm K, Macpherson ME, Storm-Larsen C, Kummen M, Fevang B, et al.
212 Selective IgA deficiency in humans is associated with reduced gut microbial diversity. *J*
213 *Allergy Clin Immunol* 2019; 143:1969-71 e11.
- 214 4. Fadlallah J, El Kafsi H, Sterlin D, Juste C, Parizot C, Dorgham K, et al. Microbial ecology
215 perturbation in human IgA deficiency. *Sci Transl Med* 2018; 10.
- 216 5. Fadlallah J, Sterlin D, Fieschi C, Parizot C, Dorgham K, El Kafsi H, et al. Synergistic
217 convergence of microbiota-specific systemic IgG and secretory IgA. *J Allergy Clin Immunol*
218 2019; 143:1575-85 e4.
- 219 6. Nielsen SCA, Roskin KM, Jackson KJL, Joshi SA, Nejad P, Lee JY, et al. Shaping of
220 infant B cell receptor repertoires by environmental factors and infectious disease. *Sci Transl*
221 *Med* 2019; 11.
- 222 7. Schickel JN, Glauzy S, Ng YS, Chamberlain N, Massad C, Isnardi I, et al. Self-reactive
223 VH4-34-expressing IgG B cells recognize commensal bacteria. *Journal of Experimental*
224 *Medicine* 2017; 214:1991-2003.

225 8. Kobayashi K, Ogata H, Morikawa M, Iijima S, Harada N, Yoshida T, et al. Distribution
226 and partial characterisation of IgG Fc binding protein in various mucin producing cells and
227 body fluids. Gut 2002; 51:169-76.

228 9. Micol R, Kayal S, Mahlaoui N, Beaute J, Brosselin P, Dudoit Y, et al. Protective effect of
229 IgM against colonization of the respiratory tract by nontypeable Haemophilus influenzae in
230 patients with hypogammaglobulinemia. J Allergy Clin Immunol 2012; 129:770-7.

231

232

233

234

235

236

237

238

239

240

241

242

243

244

245

246

247

248

249

250

251

252

253

254

255

256

257

258

259
260
261

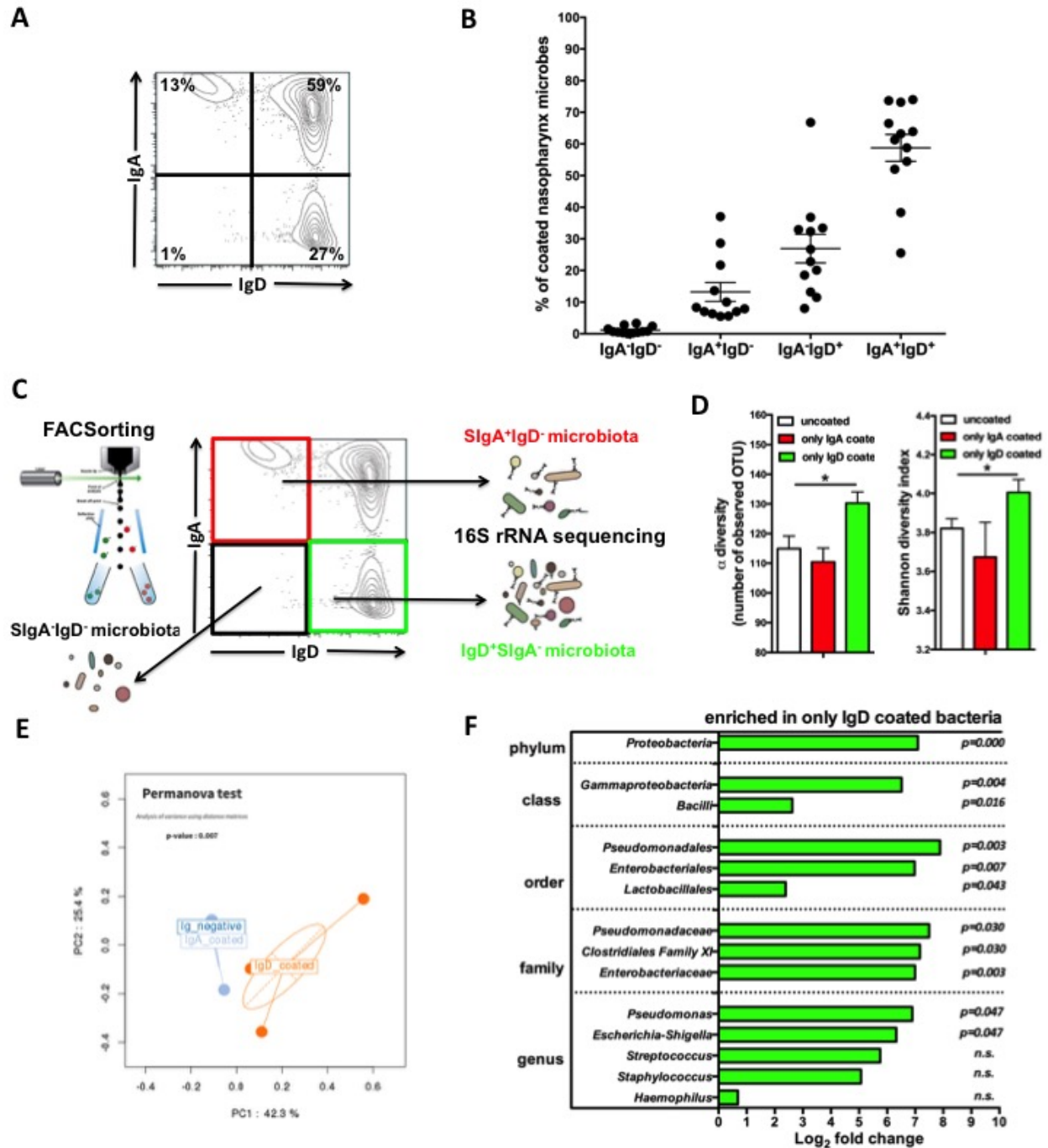
262 **FIGURE LEGENDS**

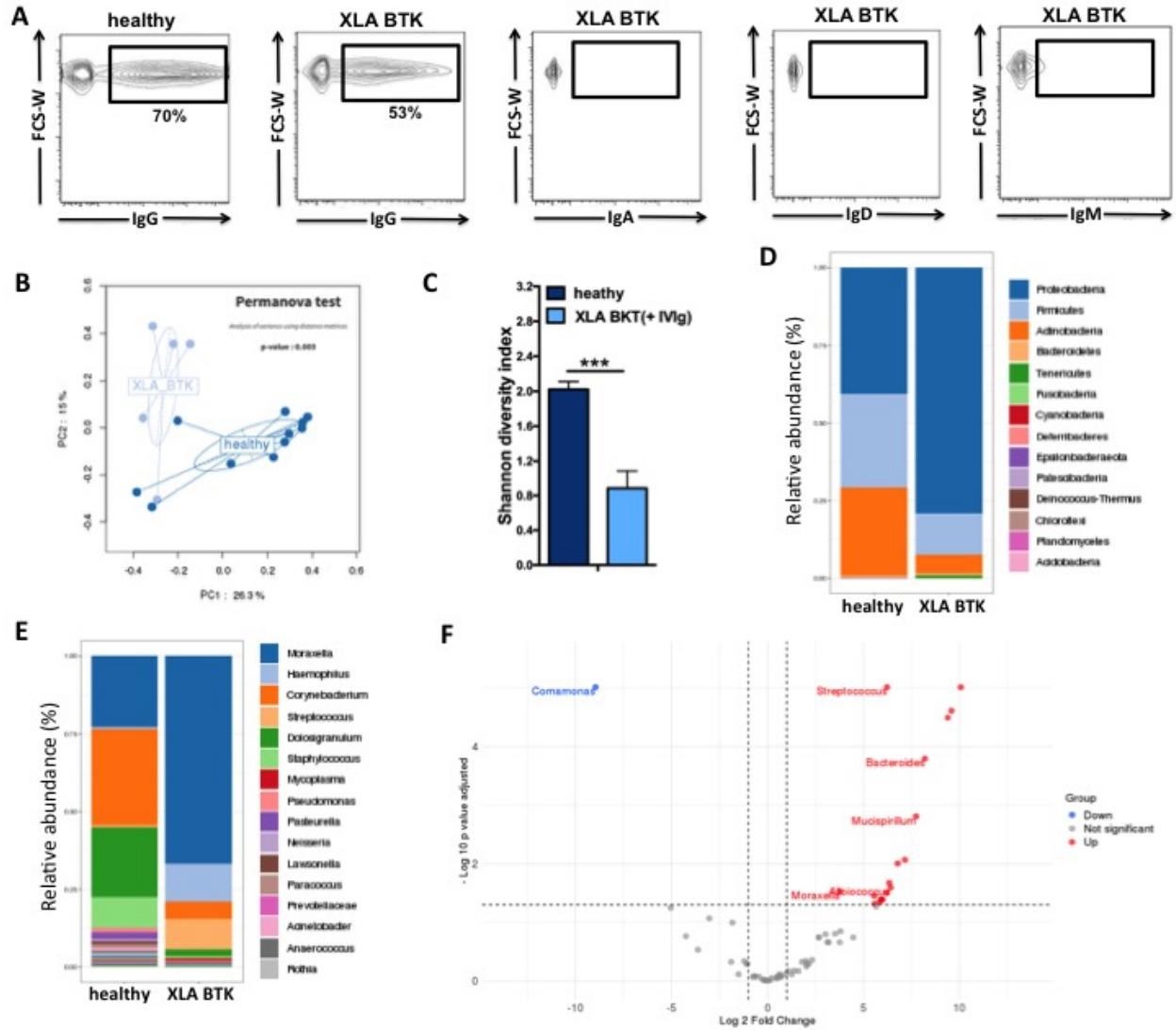
263 **FIG. 1. Nasopharynx IgD recognize a broad spectrum of pathobionts/commensals. A,**
264 Double binding of IgD and SIgA antibodies to nasopharynx microbiota. **B,** The antibody
265 binding to microbiota is highly variable between healthy subjects (n = 12). **C,** Strategy for the
266 BugFACS and 16S rRNA sequencing (n = 4). **D,** The alpha diversity, calculated using the
267 Shannon index, in different sorted fractions. Mean and standard error of mean (SEM) values
268 are indicated, and subgroups are compared with a nonparametric Mann-Whitney test. **E,**
269 Principal coordinate analysis (PCoA) of 16S RNA sequencing Operational Taxonomic Units
270 (OTU) of IgD⁺SIgA⁻ and SIgA⁺IgD⁻ sorted fraction along the first two principal coordinate
271 (PC) axes based on Bray-Curtis distance. **F,** Differential abundance analysis showing taxa at
272 phylum/class/order/family/genus level which it is found to be overrepresented in the
273 IgD⁺SIgA⁻ comparably to SIgA⁺IgD⁻ fraction.

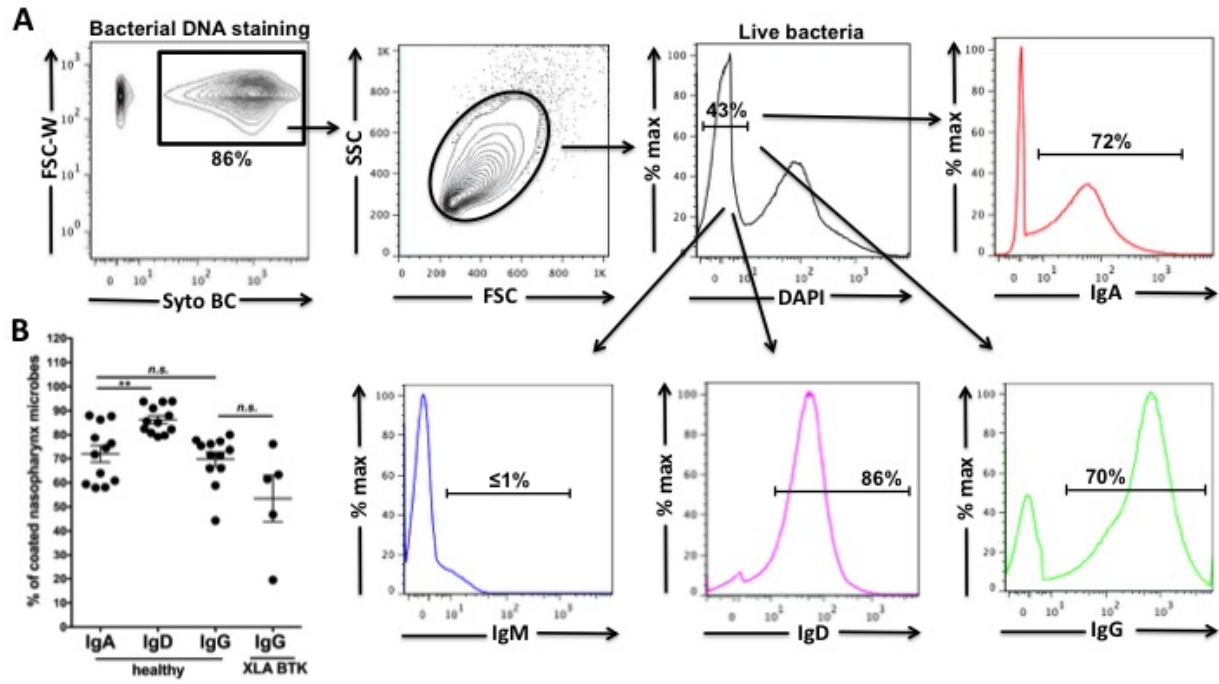
274

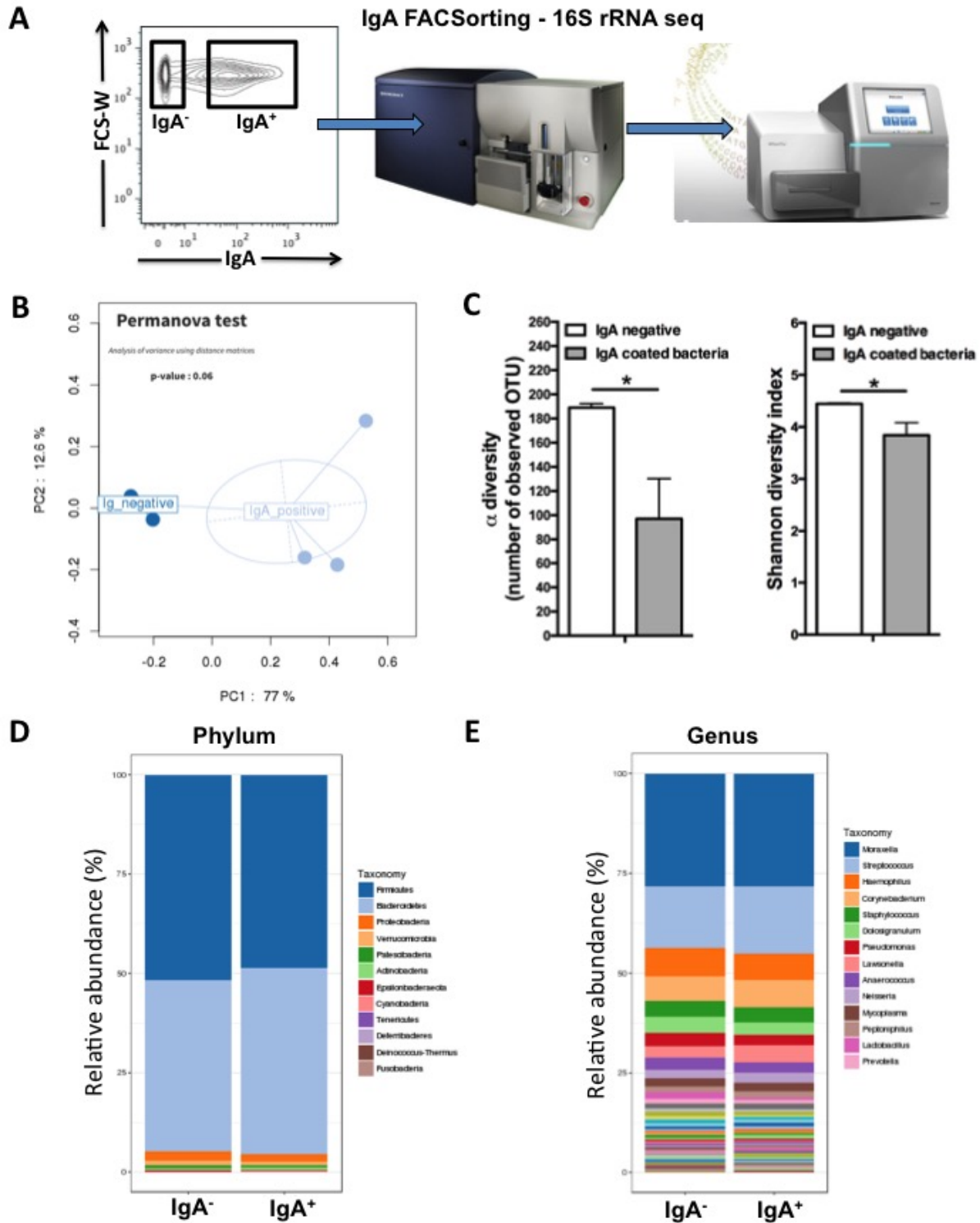
275 **FIG. 2. Immunoglobulin (IgG) replacement therapy (IVIg) “restore” the IgG binding to**
276 **pathobionts/commensals but did not rescue the nasopharynx microbiota dysbiosis of X-**
277 **linked agammaglobulinemia (XLA BTK) patients. A,** The IgG binding to nasopharynx
278 microbiota in healthy controls (n = 12) and X-linked agammaglobulinemia (XLA BTK)
279 patients under immunoglobulin (IgG) replacement therapy (n = 5). Median values are
280 indicated. **B,** Principal coordinate analysis (PCoA) of 16S RNA sequencing Operational
281 Taxonomic Units (OTU) of the healthy controls and XLA BTK patients along the first two
282 principal coordinate (PC) axes based on Bray-Curtis distances and the respective
283 PERMANOVA test. **C,** The alpha diversity, calculated using the Shannon index, in healthy
284 and XLA BTK patients. Mean and standard error of mean (SEM) values are indicated, and
285 subgroups are compared with a nonparametric Mann-Whitney test. **D, E,** Bar plot showing %
286 of microbiota phylum (**D**) and genus (**E**) level in healthy and XLA BTK patients. **F,** Volcano
287 plot displaying differential nasopharynx microbiota genus between XLA BTK patients and
288 healthy. The vertical axis (y-axis) corresponds to the mean expression value of log₁₀ (q-
289 value), and the horizontal axis (x-axis) displays the log₂ fold change value. The red dots
290 represent the up-regulated genus in XLA BTK patients; the blue dots represent the genus
291 downregulated. Positive x-values represent up-regulation and negative x-values represent
292 down-regulation.

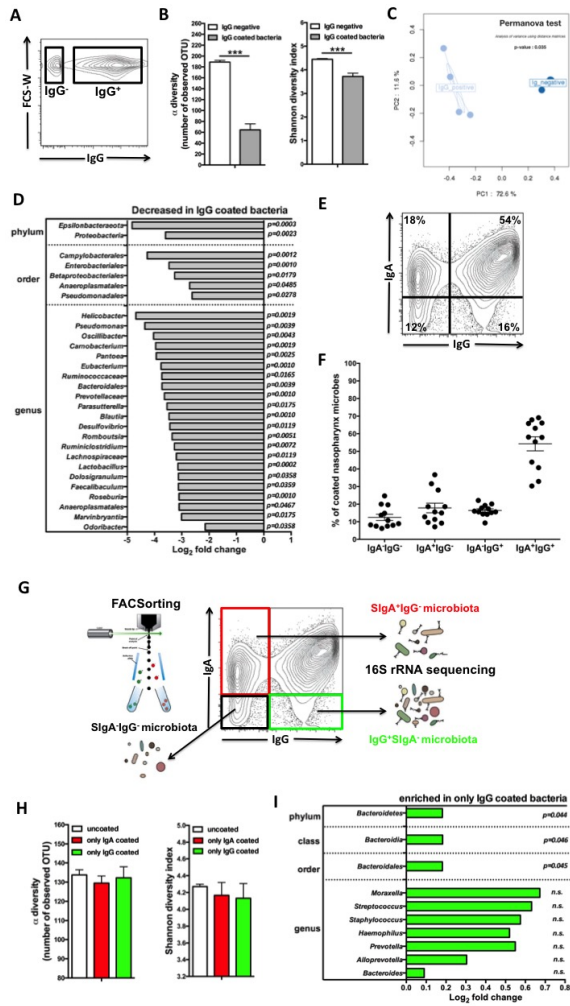
Journal Pre-proof











1 **FIG. E1. A, Gating strategy for the microbiota flow cytometric assay.** We used the DNA
2 dye SYBR Green to preferentially stain microbes allowing us to gate on (SYBR^{hi}). We then
3 used specific secondary antibodies to characterize the anti-commensal antibody (IgA, IgM,
4 IgD and IgG) response. **B,** The antibody binding to microbiota is highly variable between
5 healthy subjects (n = 12) and X-linked agammaglobulinemia (XLA-BTK) patients under
6 immunoglobulin (IgG) replacement therapy (n = 5). Median values are indicated, and
7 subgroups are compared with a nonparametric Mann-Whitney test.

8

9 **FIG. E2. Nasopharynx SIgA binds a broad spectrum of pathobionts/commensals.**

10 **A,** Strategy for the IgA-BugFACS and 16S rRNA sequencing. **B,** Principal coordinate
11 analysis (PCoA) of 16S RNA sequencing Operational Taxonomic Units (OTU) of IgA⁺ and
12 IgA⁻ sorted fraction along the first two principal coordinate (PC) axes based on Bray-Curtis
13 distance and the respective PERMANOVA test. **C,** The alpha diversity, calculated using the
14 Shannon index, in IgA⁺ and IgA⁻ sorted fraction. Mean and standard error of mean (SEM)
15 values are indicated, and subgroups are compared with a nonparametric Mann-Whitney test.
16 **D,** Bar plot showing % of microbiota phylum in IgA⁺ and IgA⁻ sorted fraction. **E,** Bar plot
17 showing % of microbiota genus in IgA⁺ and IgA⁻ sorted fraction. Data are representative of 4
18 healthy individuals.

19

20 **FIG. E3. Nasopharynx IgG recognize a broad spectrum of pathobionts/commensals. A,**
21 Strategy for the IgG-BugFACS sorting (n = 4). **B,** The alpha diversity, calculated using the
22 Shannon index, in IgG⁺ and IgG⁻ sorted fraction. Mean and standard error of mean (SEM)
23 values are indicated, and subgroups are compared with a nonparametric Mann-Whitney test.
24 **C,** Principal coordinate analysis (PCoA) of 16S RNA sequencing Operational Taxonomic
25 Units (OTU) of IgG⁺ and IgG⁻ sorted fraction along the first two principal coordinate (PC)
26 axes based on Bray-Curtis distance and the respective PERMANOVA test. **D,** Differential
27 abundance analysis showing taxa at phylum/order/genus level which it is found to be
28 downrepresented in the IgG⁺ comparably to IgG⁻ fraction. **E,** Double binding of SIgA and
29 IgG antibodies to nasopharynx microbiota. **F,** The antibody binding to microbiota is highly
30 variable between healthy subjects (n = 12). **G,** Strategy for the BugFACS and 16S rRNA
31 sequencing (n = 4). **H,** The alpha diversity, calculated using the Shannon index, in different
32 sorted fractions. Mean and standard error of mean (SEM) values are indicated, and subgroups
33 are compared with a nonparametric Mann-Whitney test. **I,** Differential abundance analysis

34 showing taxa at phylum/class/order level which it is found to be overrepresented in the
35 IgG⁺SIgA⁻ comparatibly to SIgA⁺IgG⁻ fraction.

36

37

38

39

40

41

42

Journal Pre-proof

1 METHODS

2 Patient recruitment, sample collection and processing

3 Nasopharynx specimens were obtained with sterile dry swabs (COPAN LQ Stuart
4 Transport Swab; COPAN Italia S.p.A, Brescia, Italy), which are rotated five times around the
5 inside of each nostril while applying constant pressure. Nasopharynx swabs were collected in
6 the office under strict aseptic conditions with sterile gloves and instrumentation. Laboratory
7 protocols were standardized and staff members were trained in sample preparation protocols
8 ¹. All swabs will be frozen (-80°C) upon collection from healthy individuals at local site. The
9 12 healthy donors were recruited originally as part of the *Milieu Intérieur* cohort ¹ (BioTrial,
10 Rennes, France), but were technically excluded from the main cohort due to blood sampling
11 criteria. The clinical study was approved by the Comité de Protection des Personnes - Ouest
12 6 (Committee for the protection of persons) on 13 June 2012 and by the French Agence
13 Nationale de Sécurité du Médicament (ANSM) on 22 June 2012. The study is sponsored by
14 the Institut Pasteur (Pasteur ID-RCB Number: 2012-A00238-35) and was conducted as a
15 single center study without any investigational product. The protocol is registered under
16 ClinicalTrials.gov (study# NCT01699893). X-linked agammaglobulinemia patients were
17 recruited at Hôpital Necker-Enfants Malades (French National Reference Center for Primary
18 Immunodeficiencies). Pathogenic mutations in the Bruton tyrosine kinase (BTK) were
19 identified in all 5 cases. At diagnosis, they had IgG plasma levels below 100 mg/ml with no
20 detectable IgA and IgM, while all 5 had no detectable blood B cells (CD19⁺). At time of
21 study, patients were aged 14 to 28 years (median 15). They were receiving regular IgG
22 substitution with a through level above 800 mg/dl (800 to 1385). None had antibiotic therapy.
23 Two are perfectly healthy while 3 have minimal bronchiectasis. Most recent immunological
24 investigations were unremarkable a part for the absence of detectable B cells. The age and
25 gender is not significantly different between X-linked agammaglobulinemia patients and
26 healthy. Written informed consent was obtained from all patients and/or parents. The work
27 described has been carried out in accordance with The Code of Ethics of the World Medical
28 Association (Declaration of Helsinki) for experiments involving humans.

29

30 Nasopharynx swabs processing

31 Swabs were thawed and vortexed for 1 minute at 2500 rpm to insure complete sample
32 recovery. Samples was transferred in a 96 well deep-well plate and centrifuged at 16.000g for
33 10 minutes at 4°C to pellet cells and accompanying microbes. Supernatants were recovered
34 and stored at -80°C until analysis using a TECAN Evo 75 robot.

35 **Bacterial Flow Cytometry**

36 Bacterial species-specific antibody against microbiota were assessed by a flow
37 cytometry assay was described previous². Briefly, the bacterial pellet was washed and
38 resuspended in flow cytometry buffer (1x-PBS, 2% BSA, 0.02% w/v sodium azide) with
39 SYBR Green (1/10000 (v/v) dilution, Invitrogen) incubated 30 min on ice. After, bacterial
40 suspension was washed twice and pelleted by centrifugation at 16.000g for 10 min.
41 Supernatant was removed and pellets were resuspended in 100 μ L flow cytometry buffer with
42 mouse anti-human IgA-PE (clone IS11-8E10), anti-human IgD-PerCP-Cy5.5 (clone IAG-2),
43 anti-human IgM-APC (clone SA-DA4) and anti-human IgG-BUV395 (clone G18-145) at a
44 final IgG concentration of 10 μ g/mL in a 96-well V-bottom plate and incubated for 20 min on
45 ice. Suspensions were washed once with 100 μ L of flow cytometry buffer and cells pelleted
46 by centrifugation, then resuspended in flow cytometry buffer with DAPI (Life Technologies)
47 prior to flow cytometry. Acquisition of cells events was performed using a FACS
48 LSRFortessa (Becton Dickinson, Franklin Lakes, NJ, USA) and analysis was performed with
49 Flow-Jo software software (TreeStar, Ashland, OR). Staining of live bacteria was visualized
50 by gating on SYTO BC⁺FSC⁺SSC⁺ DAPI cells.

51

52 **BugFACS**

53 Different immunoglobulin-binding microbiota were sorted³ (purity \geq 99%) using a
54 FACSaria II (BD Biosciences) into eppendorf tube in a laminar flow biocontainment hood
55 (BioProtect IV Safety Cabinet, Baker Co.). The gating strategies used to collect different
56 bacterial populations are shown in Fig. E1. Threshold settings were set to the minimal
57 allowable voltage for sidescatter (SSC). Isolated bacteria were pelleted (15.000 \times g, 10
58 minutes, 4 °C) and frozen at -80°C before sequencing of bacterial 16S rRNA genes.

59

60 **Bacterial DNA isolation and 16S rDNA sequencing**

61 In our study, we are performing the extraction of total genomic DNA from swabs
62 samples, using the TECAN Freedom EVOware workstation, and the NucleoSpin® 96
63 Genomic DNA kit (Macherey-Nagel ®). For DNA extraction, a "negative" control was
64 included containing buffers. Briefly, the pellets that remain in the deep well plate were
65 incubated with Ready-Lyse™ Lysozyme Solution (250 U/ μ L) (Epicentre, Hessisch Oldendorf,
66 Germany) for 30 minutes at 37°C. Next, we incubated the suspension with Proteinase
67 K/buffer T1 working solution at 55°C overnight until the samples are completely lysed. We
68 add 20 μ g of glycogen (DNA carrier) and we follow the DNA extraction kit protocol. Finally

69 we eluted the DNA in 25 µl and the DNA box is immediately frozen at -80°C at local center
70 until its use. The concentration of extracted DNA is determined using TECAN (QuantiFluor®
71 ONE dsDNA System, Promega), and DNA integrity and size were also confirmed with the
72 Agilent 2100 Bioanalyzer (Agilent Technologies, USA). The V3-V4 region of the bacterial
73 16S rRNA region were PCR amplified with V3-340F (CCTACGGRAGGCAGCAG) and
74 V4-805R (GGACTACHVGGGTWTCTAAT) containing a primer linker, primer pad, unique
75 8-mer Golay barcode which was used to tag PCR products from respective samples and
76 negative control. PCR reactions consisted of 18 µl of AccuPrime Pfx SuperMix (12344-040;
77 Invitrogen), 0.5 µl of each primers and 1 µl of DNA (10 ng). PCR was carried out as follows:
78 95 °C for 2 min, 30 cycles of 95 °C for 20 s, 55 °C for 15 s and 72 °C for 1 min, and a final
79 extension step at 72 °C for 10 min on a Biorad thermocycler. PCR products were cleaned
80 using NucleoMag magnetic purification beads (MACHEREY-NAGEL Kit) following the
81 protocol, quantified with the QuantiFluor® ONE dsDNA kit (Promega), and pooled in equal
82 amounts of each PCR product. Library pools were loaded at 12pM with a 15% PhiX spike for
83 diversity and sequencing control, onto a v3 300-bp paired end reads cartridge for sequencing
84 on the Illumina MiSeq NGS platform.

85

86 **Sequence processing and statistical analysis**

87 After removing reads containing incorrect primer or barcode sequences and sequences
88 with more than one ambiguous base, we recovered from 53 samples a total of 3.090.252 reads
89 (58.307 reads on average). The bioinformatics analysis was performed as previously
90 described ⁴. Briefly, amplicons were clustered into operational taxonomic units (OTU) with
91 VSEARCH (v1.4) and aligned against the SILVA database. The input amplicons were then
92 mapped against the OTU set to get an OTU-abundance table containing the number of reads
93 associated with each OTU. The normalization, statistical analyses and multiple visualization
94 were performed with SHAMAN (SHiny application for Metagenomic Analysis
95 (shaman.c3bi.pasteur.fr) based on R software.

96

97 **Statistical analysis**

98 GraphPad Prism was used for statistical analysis. Thus, non-parametric tests (Mann
99 Whitney U-test) were used where applicable.

100

101

102

103 **METHOD REFERENCES**

- 104 1. Thomas S, Rouilly V, Patin E, Alanio C, Dubois A, Delval C, et al. The Milieu Interieur
 105 study An integrative approach for study of human immunological variance. *Clinical*
 106 *Immunology* 2015; 157:277-93.
- 107 2. Moor K, Fadlallah J, Toska A, Sterlin D, Balmer ML, Macpherson AJ, et al. Analysis of
 108 bacterial-surface-specific antibodies in body fluids using bacterial flow cytometry. *Nat Protoc*
 109 2016; 11:1531-53.
- 110 3. Palm NW, de Zoete MR, Cullen TW, Barry NA, Stefanowski J, Hao L, et al.
 111 Immunoglobulin A coating identifies colitogenic bacteria in inflammatory bowel disease. *Cell*
 112 2014; 158:1000-10.
- 113 4. Quereda JJ, Dussurget O, Nahori MA, Ghozlane A, Volant S, Dillies MA, et al. Bacteriocin
 114 from epidemic *Listeria* strains alters the host intestinal microbiota to favor infection.
 115 *Proceedings of the National Academy of Sciences of the United States of America* 2016;
 116 113:5706-11.

117

118 Author: The Milieu Intérieur Consortium[†].

119

120 [†] The Milieu Intérieur Consortium[¶] is composed of the following team leaders:
 121 Laurent Abel (Hôpital Necker), Andres Alcover, Hugues Aschard, Kalla Astrom (Lund
 122 University), Philippe Bousso, Pierre Bruhns, Ana Cumano, Caroline Demangel, Ludovic
 123 Deriano, James Di Santo, Françoise Dromer, Gérard Eberl, Jost Enninga, Jacques Fellay
 124 (EPFL, Lausanne), Odile Gelpi, Ivo Gomperts-Boneca, Milena Hasan, Serge Herberg
 125 (Université Paris 13), Olivier Lantz (Institut Curie), Claude Leclerc, Hugo Mouquet, Sandra
 126 Pellegrini, Stanislas Pol (Hôpital Cochin), Antonio Rausell (INSERM UMR 1163 – Institut
 127 Imagine), Lars Rogge, Anavaj Sakuntabhai, Olivier Schwartz, Benno Schwikowski, Spencer
 128 Shorte, Frédéric Tangy, Antoine Toubert (Hôpital Saint-Louis), Mathilde Trouvier
 129 (Université Paris 13), Marie-Noëlle Ungeheuer, Matthew L. Albert (In Vitro)[§], Darragh
 130 Duffy[§], Lluís Quintana-Murci[§],

131

132 [¶] unless otherwise indicated, partners are located at Institut Pasteur, Paris133 [§] co-coordinators of the Milieu Intérieur Consortium

134

135 Additional information can be found at: <http://www.pasteur.fr/labex/milieu-interieur>

136